Structural signatures of (two) characteristic dynamical temperatures in lithium metasilicate

2014 J. Phys.: Condens. Matter 26 155104

(http://iopscience.iop.org/0953-8984/26/15/155104)

IOP Publishing Journal of Physics: Condensed Matter
J. Phys.: Condens. Matter **26** (2014) 155104 (8pp) doi:10.1088/0953-8984/26/15/155104

Structural signatures of (two) characteristic dynamical temperatures in lithium metasilicate

Cristian Balbuena[1], Carolina Brito[2] and Daniel A Stariolo[2]

[1] Universidad Nacional del Sur, Departamento de Química INQUISUR, Avenida Alem 1253, 8000-Bahía Blanca, Argentina
[2] Departamento de Física, Universidade Federal do Rio Grande do Sul, CP 15051, 91501-970 Porto Alegre, RS, Brazil

E-mail: daniel.stariolo@ufrgs.br

Received 13 October 2013, revised 16 December 2013
Accepted for publication 24 January 2014
Published 27 March 2014

Abstract

We report on the dynamic and structural characterization of lithium metasilicate Li_2SiO_3, a network-forming ionic glass, by means of molecular dynamics simulations. The system is characterized by a network of SiO_4 tetrahedra disrupted by Li ions which diffuse through the network. Measures of mean square displacement and the diffusion constant of Si and O atoms allow us to identify the mode-coupling temperature, $T_c \approx 1500$ K. At a much lower temperature, a change in the slope of the specific volume versus temperature singles out the glass transition at $T_g \approx 1000$ K, the temperature below which the system goes out of equilibrium. We find signatures of both dynamical temperatures in structural order parameters related to the orientation of the tetrahedra. At lower temperatures we find that a set of order parameters which measure the *relative orientation* of neighbouring tetrahedra cease to increase and stay constant below T_c. Nevertheless, the bond orientational order parameter, which in this system measures local tetrahedral order, is found to continue growing below T_c until T_g, below which it remains constant. Although these structural signatures of the two dynamical temperatures do not imply any real thermodynamic transition in terms of the order parameters, they do give insight into the relaxation processes that occur between T_c and T_g, in particular they allow us to characterize the nature of the crossover happening around T_c.

Keywords: glass transition, mode-coupling theory, molecular dynamics simulations, silicate glasses

(Some figures may appear in colour only in the online journal)

1. Introduction

Silicate oxide glasses are the most used and studied kind of inorganic glasses. They have many applications ranging from window glasses to optical fibres [1]. Typically, the local structure of these systems are tetrahedra of silicon (Si) and oxygen (O) atoms, which are connected to form a network. The presence of lithium atoms (Li), which are called modifying cations, disrupts the connectivity of some tetrahedra and is responsible for important physical properties of the system, as for example electric conduction [1–3]. SiO_4 tetrahedra are formed at a sufficiently high temperature, where they diffuse together with the free Li atoms. This is the liquid state of lithium metasilicate Li_2SiO_3. As the temperature decreases, the Si and O atoms slow down until a temperature T_g where both atoms stop diffusing, although the Li ions keep travelling in the network of tetrahedra. This happens at the glass transition temperature T_g, at which the relaxation times of Si and O rise beyond accessible laboratory time scales. Below T_g the system displays an ionic glass phase.

In the last decades much effort has been made to understand the nature of the glass transition and characterize the glassy phase in many different systems [1, 4–6]. One important question is if there is any structural signature accompanying the strong slowing down of the dynamics as the system approaches the glass transition. While there is no definitive answer to this question yet, the search for such structural signatures (besides the obvious relevance to the whole picture of the glass transition) is important as it gives new insights into the nature of the slowing down [7]. Among theoretical approaches, an important reference has been the mode-coupling theory (MCT) [8]. MCT accounts well for some aspects of the initial slowing down of the dynamics, in particular the appearance of a two-step relaxation of correlations with a non-trivial short time β regime and a structural, long time α regime [8–10]. It predicts a critical-like divergence of relaxation times at a characteristic temperature $T_c > T_g$. Nevertheless, it is well known that in real systems there is no actual divergence of relaxation times at T_c, which has to be interpreted as a crossover temperature from a relatively fast relaxation regime to a much slower one.

Systems like lithium metasilicate have a local structure given by a network of tetrahedra. The short-range order of tetrahedra is very robust, even in the liquid phase, posing strong orientational constraints to relaxation. In this case, it is important to use a description that is able to capture this short-range order and analyse its influence on the dynamical properties of the system.

In this work we report a molecular dynamics study of the dynamical and structural properties of Li_2SiO_3 using two complementary approaches. (i) We first analyse the dynamics by measuring the mean square displacement of each kind of atom and the self-correlation function of its positions. We measure the diffusion coefficient D and relaxation times, which allow us to define the critical mode-coupling temperature T_c, i.e. the temperature at which the extrapolated D of the Si and O atoms goes to zero. The crossover nature of this transition is evident in our results, which show a continuously relaxing system even below T_c, as will be discussed below. At a much lower temperature, T_g, we observe a change in the slope of the specific volume versus temperature curve where the systems falls out of equilibrium, signalling a glass transition. For $T < T_g$ the dynamics shows ageing and it is not possible to equilibrate the system within the available computer time. (ii) We also measured two orientational quantities. The first quantity is the bond orientational or Steinhardt order parameters, from which it is possible to identify the local structure of the network [11]. To go beyond this local measure we computed a set of recently defined quantities, called the 'Rey parameters' [12], which quantify the relative orientations of nearby tetrahedra. We find that the two characteristic temperatures extracted from dynamics, namely T_c and T_g, have counterparts in the behaviour of the orientational parameters: T_c corresponds to the temperature below which the relative orientation *between* tetrahedra (Rey parameters) remains fixed, while the system is still relaxing at the atomic level, as made evident from the growth in the bond orientational parameters for $T_g < T < T_c$. In turn, T_g corresponds to the temperature below which the average positions of the atoms that make up the tetrahedra freeze in the time scales of the simulations.

The paper is organized as follows: in section 2 we define the model and details of the molecular dynamics protocol. In section 3 we analyse the dynamics of the system in the context of mode-coupling theory. In section 4 we define and analyse orientational order parameters. In section 5 we end with a discussion of our results.

2. The model

We have performed classical molecular dynamics simulations of Li_2SiO_3 containing $N = 3456$ particles, of which $N_{Li} = 1152$, $N_{Si} = 576$, $N_O = 1728$ correspond to Li, Si and O atoms, respectively. The interaction potential was chosen to be of the Gilbert–Ida type [13] with a r^6 term:

$$U_{ij} = \frac{e^2}{4\pi\epsilon_0}\frac{q_i q_j}{r} - \frac{c_i c_j}{r^6} + f_0(b_i + b_j)\exp\left[\frac{a_i + a_j - r}{b_i + b_j}\right] \quad (1)$$

where the pair of indices i, j characterizes different pairs Li–Li, Li–Si, Li–O, etc and r is the corresponding distance. The first term in (1) is the Coulomb interaction with the effective charges q_i for Li, Si and O. The long-range nature of the Coulomb interaction was taken into account by means of the Ewald summation method [14, 15]. The second term is a dispersive interaction and the last term is a Born–Meyer type potential that accounts for repulsive short-range interactions. The potential parameters were attributed on the basis of *ab initio* molecular orbital calculations [16, 19]. Their validity was checked in the liquid, glassy and crystal states under constant pressure conditions showing good agreement with experimental data [17, 18]. The simulations were implemented with the software LAMMPS [20], and a Verlet algorithm with a time step of 1 fs was used to integrate the equations of motion [14, 15]. The box size was determined by performing simulations in the NPT ensemble at atmospheric pressure, which allows us to reach the same density as the experimental data for any temperature within the experimental error.

The system was equilibrated at 3500 K for more than 0.5 ns, starting from a random configuration, using the NVE ensemble. After that, the temperature was decreased until 3200 K followed by 2 ns in NPT, 1 ns in NVE and 1 ns in the NVT ensemble to ensure the absence of a drift in pressure and temperature. Then, the system was equilibrated in a 2 ns run using the NVE ensemble. Finally, after this equilibration procedure, trajectories of 1–10 ns were generated in the NVE ensemble for analysis [14, 15].

In this work we present simulations for a wide range of temperatures, 600 K $\leq T \leq$ 3200 K. At each temperature the system was equilibrated following the same protocol before starting the production run.

Structurally, ionic silicates are formed by a network of SiO_4 tetrahedra in which Si is surrounded by four O atoms, disrupted by the presence of modifier alkali atoms. The glassy matrix is a result of the chain formation of these

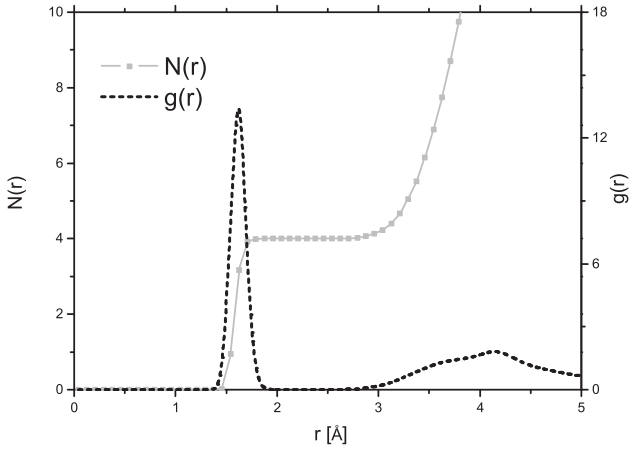

Figure 1. The radial distribution function $g(r)$ for Si–O pairs in lithium metasilicate and the coordination number $N(r)$.

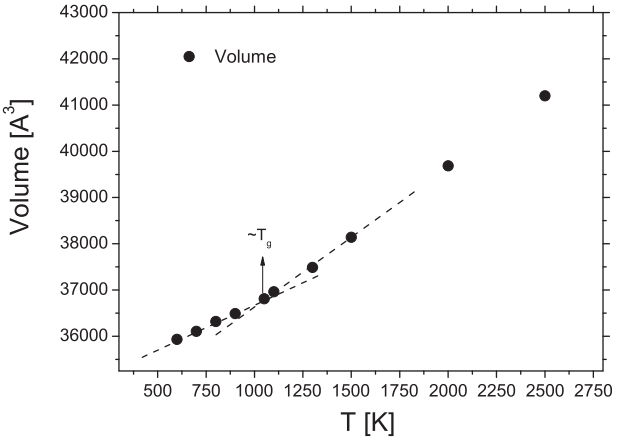

Figure 2. Specific volume as a function of temperature. A change in the slope of the curve occurs at $T_g \approx 1000$ K signalling a glass transition.

tetrahedra sharing their apses (bridging oxygens (BO)). The incorporation of a small amount of Li_2O (modifier oxide) does not destroy the SiO_4 tetrahedra but replaces a covalent bridge (BO) by non-bridging oxygen atoms (NBO) [21]. In figure 1 we show the radial distribution function (RDF) $g(r)$ between Si and O atoms. The integral of $g(r)$ gives the coordination number of the Si atoms:

$$N(r) = 4\pi\rho \int_0^r r^2 g(r)\, \mathrm{d}r, \tag{2}$$

where the existence of four neighbouring O atoms is evident.

3. Dynamic characterization of lithium metasilicate

Our simulations show the presence of a glass transition at $T_g \approx 1000$ K, as can be seen in figure 2 by the change in the slope of the specific volume as function of temperature. Similar results have been obtained by other authors [18, 22]. At this temperature the system goes out of equilibrium. We verified this by noting, among other signatures, the presence of ageing effects in relaxation functions. Instead, for $T > T_g$ we were able to equilibrate the system within the available simulation time.

Changes in the structure of the system for the range of temperatures studied were monitored through the RDF $g(r)$. As can be seen in figure 3(left), the RDF for Si–O has one large peak which corresponds to the distance between a Si atom and its first neighbour O atom that form the tetrahedral structure. Note that the Si–O RDF changes very little with temperature over the whole temperature range, signalling the robustness of the tetrahedra. The RDFs of Si–Si (figure 3(centre)) and Si–Li (figure 3(right)) pairs have well defined peaks, reminiscent of a periodic solid structure.

From the behaviour of the RDF one can conclude that there are no strong structural changes over the wide range of temperatures studied, in particular around the glass transition temperature T_g. In spite of this structural robustness, the dynamical behaviour of the three types of atoms is very different. In these super-ionic glass formers the alkali atoms move on a timescale which is, at low temperatures, many orders of magnitude faster than that for the atoms constituting the matrix (Si and O). In figure 4 the mean squared displacement (MSD) of O, Si and Li atoms is shown. The different time scales for relaxation for the matrix and Li atoms is evident.

MCT has been used to rationalize several dynamical characteristics of ionic silicates [4, 8, 17, 23]. When it applies, a distinctive prediction of MCT is a diffusional arrest at a characteristic temperature T_c, which is usually above the corresponding glass transition temperature T_g. The theory predicts a power law divergence of the structural relaxation time τ and a corresponding dropping of the diffusion constant to zero with the same power law, i.e. with a common exponent γ [8]:

$$D(T) \propto (T - T_c)^{\gamma} \tag{3}$$

$$\tau(T) \propto (T - T_c)^{-\gamma}. \tag{4}$$

We have extracted relaxation times from the relaxation of the incoherent intermediate scattering function defined as

$$F_s^{\delta}(\vec{k}, t) = \frac{1}{N} \sum_{i=1}^{N_\delta} \langle \exp\left[\mathrm{i}\vec{k} \cdot (\vec{r}_i(t) - \vec{r}_i(0))\right] \rangle \tag{5}$$

where the index δ labels the different species of atoms. For isotropic systems, $F_s^{\delta}(k, t)$ depends only on the modulus of the wavevector. In figure 5 $F_s^{\delta}(k, t)$ are shown for Si and O atoms at different temperatures above T_g. The wavevector was chosen to be $k = 2.1$ Å^{-1}, which corresponds to the nearest-neighbour distance between Si atoms. The relaxation time τ was defined as the time at which $F_s^{\delta}(k, t)$ decays to 0.1. Figure 6 shows the temperature dependence of the diffusion constant and the structural relaxation time for Si and O atoms. The inset of figure 6 shows that $D(T)$ and $\tau(T)$ obey a common power law scaling for a range of temperatures, as expected by MCT. Linear fits to these data give a value of the exponent $\gamma \approx 2.5$. We verified that this value is robust for other values of the wavevector k. In the main figure we show that extrapolation of the data to low temperatures results in a point at which all data sets intersect at a characteristic temperature $T_c \sim 1500$ K. We then associate this T_c with the mode-coupling temperature

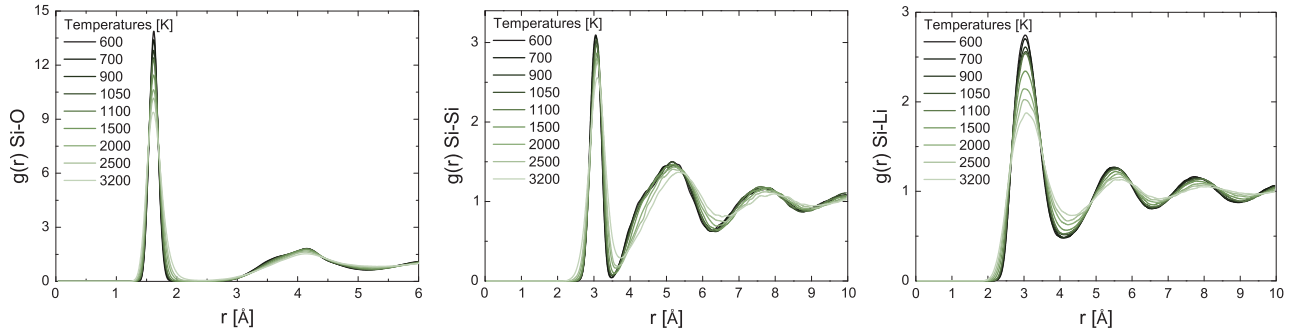

Figure 3. Radial distribution function between different species of atoms for the range of temperatures 600 K $\leq T \leq$ 3500 K: left, Si–O; centre, Si–Si; right, Si–Li. Asymptotically, all RDFs go to one, as expected.

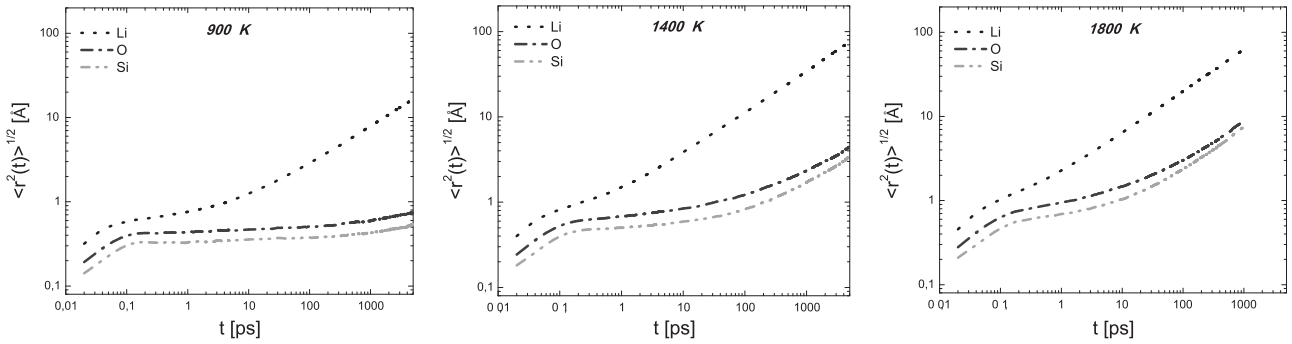

Figure 4. Mean square displacement of Si, O and Li atoms for three characteristic temperatures 900 K $\leq T_g \leq$ 1400 K $\leq T_c \leq$ 1800 K.

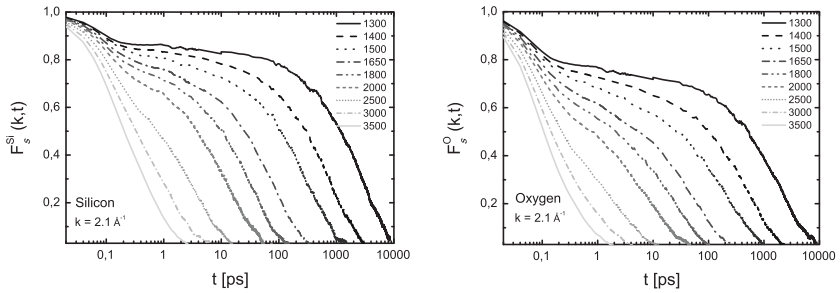

Figure 5. Self-intermediate scattering function of Si (left) and O (right) atoms for different temperatures and a common wavevector (see text).

of the system, as discussed above. Nevertheless, note that the behaviour of the relaxation times and diffusion constant already departs from a power law at temperatures $T > T_c$.

We conclude this section noting that it is possible to identify at least two characteristic temperatures of the system where the dynamics goes through qualitative changes: the glass transition temperature $T_g \sim 1000$ K, which is the temperature at which the system falls out of equilibrium in the accessible time scales of the simulation, and the mode-coupling temperature, $T_c \sim 1500$ K, which is frequently interpreted as signalling the dominance of an activated dynamics [24, 25]. We have also verified that no structural signal of these dynamical transition temperatures is observed in the radial correlation functions, as usual. In section 4 we show that it is possible to characterize the mode-coupling crossover from the change in behaviour of static (equilibrium) orientational order parameters.

4. Orientational measures

4.1. Local orientational order around Si atoms

Local orientational order can be determined by the Steinhardt or bond orientational order parameters (BOO) defined as [11]:

$$Q_l = \left[\frac{4\pi}{2l+1} \sum_{m=-l}^{l} |\bar{Q}_{lm}|^2 \right]^{1/2}, \qquad (6)$$

where $\bar{Q}_{lm} = \langle Q_{lm}(\vec{r}) \rangle$ and $Q_{lm}(\vec{r}) = Y_{lm}(\theta(\vec{r}), \phi(\vec{r}))$ are spherical harmonics with $\theta(\vec{r})$, $\phi(\vec{r})$ the polar angles of a bond measured with respect to some reference coordinate system and where the average is taken over some suitable set of bonds. A 'bond' is a line that connects the centres of two neighbouring atoms. The matrix of tetrahedra in Li_2SiO_3 is disordered in the

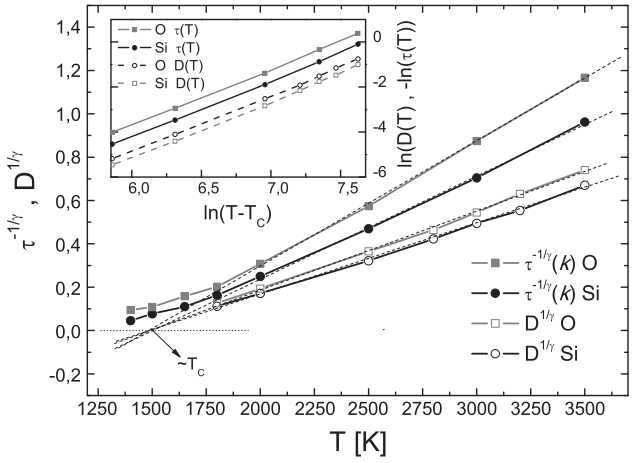

Figure 6. Scaled diffusion constant and structural relaxation time of Si and O atoms versus temperature. The (extrapolated) intersection defines the mode-coupling critical temperature. Inset: the same data in a log–log scale which show good agreement with the power laws predictions of MCT (see text). The diffusion coefficients are very similar to the ones that are reported in [18].

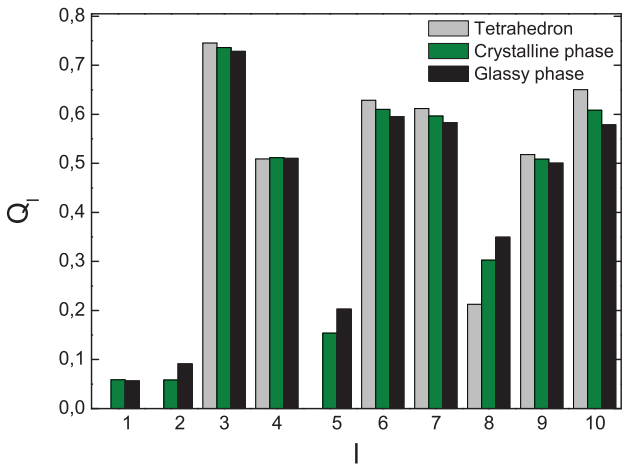

Figure 7. Bond orientational order parameters Q_i for $i = 1, \ldots, 10$ comparing a perfect tetrahedron, a tetrahedron from the crystalline cell of the system and one in the low temperature glass phase at $T = 600$ K.

sense of simple crystalline order, and we do not expect to obtain meaningful information computing BOO parameters beyond first or second neighbours. Nevertheless, they can give valuable information on the evolution with temperature of short-range order, i.e. tetrahedra.

In this work we considered BOO of the neighbourhood of Si atoms, as determined by the first peak of the $g(r)$ of Si–O. Figure 7 shows a bar plot with the values of Q_l from $l = 1$ to $l = 10$ comparing three different systems: a perfect tetrahedron, the crystalline structure of the system [26] and the glass structure of metasilicate at $T = 600$ K. The small differences in Q_l values between a perfect tetrahedron and SiO_4 tetrahedra in silicates is because in the latter the tetrahedra are not mutually independent (isolated)—most are linked by bridging O atoms which distort the optimal structure somewhat. The existence of such a BO type impedes the perfect orientation of individual tetrahedra, even in the crystalline phase. The dominant symmetry is given by $l = 3$ which reflects the three-fold symmetry of tetrahedra [6, 27]. In figure 8 we show how $\langle Q_3 \rangle$ evolves with temperature. Averages were taken from 30 different configurations of the whole system to improve statistics. In each configuration 576 tetrahedra (the number of Si atoms) were analysed, resulting in a total of 17 280 tetrahedra at each temperature. In figure 8(a) the lower (black) points correspond to instantaneous configurations along a molecular dynamics trajectory and the upper (red) points correspond to measures in the inherent structures from equilibrium configurations at each temperature. It can be seen that up to approximately $T \sim 900$ K both data sets behave similarly and show no variation with temperature. The system is effectively frozen in its glass phase in this regime. Above $T \sim 900$ K orientational order of instantaneous configurations decreases, signalling a change in the tetrahedron structure around Si atoms. Nevertheless, the corresponding inherent structure measures show a constant value up to $T \sim 1500$ K. This means that tetrahedra in the interval $900\ \text{K} \leq T \leq 1500$ K are robust structures, i.e. they can deform and accommodate in order to find more stable global configurations of the network, but the landscape is characterized by a common tetrahedral structure in the entire temperature range. In figure 8(b) the distribution of instantaneous Q_3 values is shown for a wide range of temperatures. The distribution is peaked around the

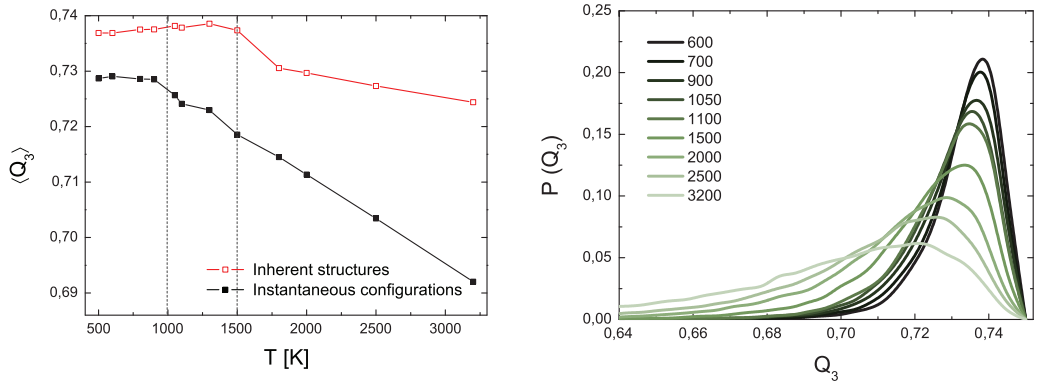

Figure 8. Left: Temperature dependence of Q_3 for instantaneous (black) and inherent structure (red) configurations. Right: distribution of instantaneous Q_3 values for different temperatures.

mean value at low temperatures and broadens, as expected, as temperature increases, but otherwise we can see no obvious signs of structural changes from the form of the distribution in a wide temperature range. This spread in the distribution of Q_3 was previously observed for Si systems in the supercooled phase [6] and used to quantify the modification of the local structure when the system experiences a phase transition. It is important to note that although the distribution of instantaneous Q_3 is large, its mean value is well defined from nearly 17 000 independent measures. If we were to plot the error bars in figure 8(a), they would be smaller than the size of the symbols. Note that for temperatures as high as 2500 K the probability of finding a tetrahedral structure of O around a Si atom is relatively high, i.e. tetrahedra are very robust structures.

4.2. Relative orientations between tetrahedra

Note that the BOO parameter Q_3 described in the previous section captures the local orientational order between a Si atom and the O atoms surrounding it. In the system under study, this amounts to characterizing the geometry of single tetrahedra for different temperatures. If one wants to go further in the characterization of orientational order it is important to understand how the tetrahedra correlate in space, how they organize relative to each other when the temperature changes. In general, if local order is simple, as is the case in simple molecular liquids forming highly symmetric crystals at low temperatures, then the spatial correlations of the BOO parameters can be used to search for medium- and long-range order in the system. In the case of Li_2SiO_3, which forms a complex silicate network of tetrahedra modified by Li ions, a useful correlation function of the local order parameter should capture the *relative orientation* between tetrahedra. To quantify this relative orientational order in tetrahedron-forming systems Rey introduced a useful quantity for the case of carbon tetrachloride [12] which we here adapt to ionic silicates.

The Rey parameters are defined as follows: take two Si atoms Si_1 and Si_2 and define the vector $\vec{r}_{12}$ that connects them. Then define the two planes passing through the Si atoms and perpendicular to $\vec{r}_{12}$. Then count how many O atoms are shared by the two Si atoms between these planes and define different 'orientational classes'. Note that, due the tetrahedral character of the network, there are a few possibilities for O-sharing configurations: if there are two O atoms between the planes, this is the 1:1 'corner-to-corner' configuration. If there are three O atoms then this is the 2:1 or 'corner-to-edge' configuration, and so on. At most, the two Si atoms can share three O atoms each, corresponding to a face of the tetrahedron. This is the 3:3 or 'face-to-face' configuration. In figure 9 we show some configurations and their respective names. Each configuration defines one class of the Rey parameters. Different from carbon tetrachloride, in which each Cl atom is connected with a single C atom, in Li_2SiO_3 a fraction of the O atoms are 'bridging', i.e. are at a vertex connecting two tetrahedra. Then, we adapted the original definition in order to accommodate this possibility: bridging O atoms are considered to belong to both Si atoms, and then counted twice in the corresponding cases.

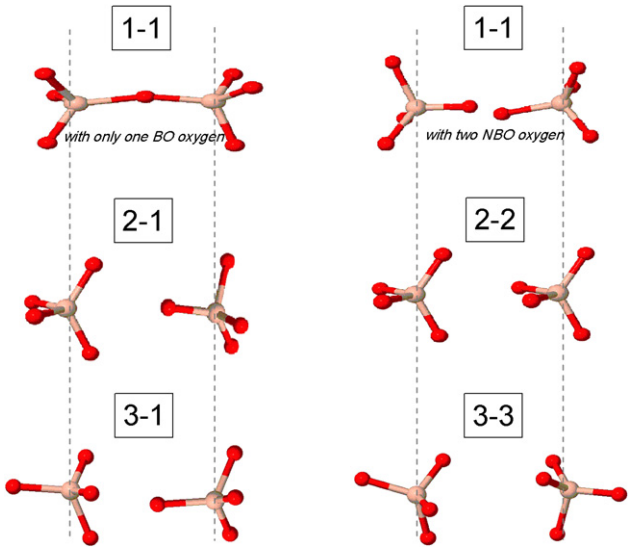

Figure 9. Definition of the *classes* of the Rey parameters. Possible relative orientations of a couple of tetrahedra showing the number of shared O atoms of the two Si atoms. Note that there are two possibilities in which two Si share one O each: a common BO and two NBOs (see text).

Figure 10 (left) shows the percentage of each class, f, as a function of the distance between Si atoms for $T = 1500$ K, together with the radial distribution function Si–Si. Within the first peak of the RDF there appear only three classes with a finite contribution: corner-to-corner (1:1), corner-to-edge (1:2) and edge-to-edge (2:2). Up to the second maximum of the RDF the relative percentages of the different classes fluctuate considerably. Nevertheless, at short distances configurations with a few sharing O atoms are favoured. In figure 10 (right) the three dominant configurations near the first peak of the RDF are shown as a function of distance between Si atoms for different temperatures. It can be seen that there are no strong qualitative variations with temperature except for a change in the height of the peaks.

Next, we address the behaviour of the Rey parameters for Si atoms at the first peak of the RDF (nearest neighbours). Figure 11 shows the temperature dependence of all classes for two nearest-neighbour Si atoms. It is evident that for two nearest-neighbour tetrahedra at any temperature $600\ \text{K} \leq T \leq 3200\ \text{K}$ the only configurations with sizeable probabilities are 1:1, 2:1 and 2:2. Furthermore, classes 1:1 and 2:1 are more probable than 2:2 at any temperature. At $T \approx 1500$ K an interesting bifurcation in the probabilities of the two more probable classes occurs. It is seen that coming from high temperatures where the probabilities of each class approach those of a random configuration of tetrahedra, the three more probable configurations change continuously until $T \sim 1500$ K, below which no more changes in the values of any of the classes are observed. Interestingly, this temperature is consistent with the mode-coupling temperature T_c found by an analysis of relaxation data. Below this temperature any two nearby tetrahedra keep their relative orientations frozen, i.e. no more orientational rearrangements occur in the network.

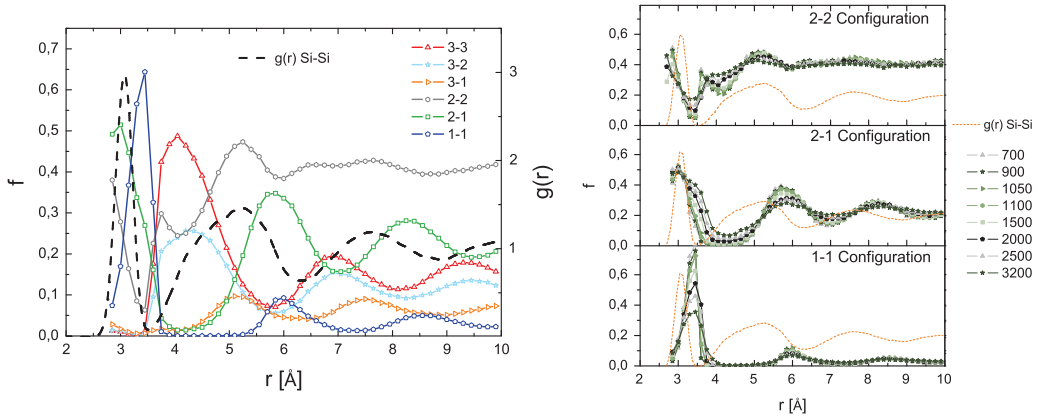

Figure 10. Left: percentages of each class of Rey parameters as function of distance at $T = 1500$ K. The RDF of Si–Si is shown (dashed) to give an idea of the distances between the Si atoms that are at the centre of the tetrahedra. Right: the most frequent Rey configurations near the first peak of the RDF for different temperatures.

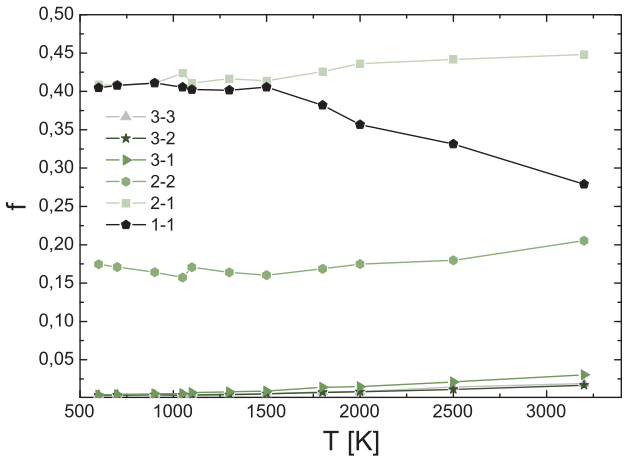

Figure 11. Variation with temperature of the percentages f of the Rey parameters for pairs of Si atoms at a distance corresponding to the first peak of the Si–Si RDF (nearest-neighbour atoms).

Note that, although this points to an orientational freezing of the local structure at $T_c \sim 1500$ K, the instantaneous BOO parameter $\langle Q_3 \rangle$ continues growing down to a much lower temperature $T \sim 900$ K, near the glass transition temperature. Nevertheless, the BOO measured for the inherent structures shows a behaviour similar to the Rey parameters, as seen in figure 8.

We finish this section by noting that for the Rey parameters for a distance corresponding to the second maximum (second neighbours) no interesting signal is evident. All classes show an approximately constant value in the whole temperature range. The values correspond roughly to a random distribution, or a 'gas' of tetrahedra [12], although for the Li_2SiO_3 system tetrahedra are never completely random because of the presence of bonding O atoms.

5. Discussion and conclusion

The results described in the previous sections are summarized in figure 12, where we show four plots comparing the outcome of dynamical and thermodynamical measures. In our simulations of lithium metasilicate we observed qualitative changes in the dynamics at two characteristic temperatures: the glass transition temperature T_g, which is detected from the discontinuity in the slope of the specific volume versus temperature, and the mode-coupling temperature T_c, defined as the temperature at which the extrapolated diffusion constant D of the Si and O atoms goes to zero. We find $T_g \approx 1000$ and $T_c \approx 1500$. Although the RDF does not present any important modification at these temperatures, we found that two types of orientational parameters do show qualitative changes at T_g and T_c. The bond orientational order parameter $\langle Q_3 \rangle$ characterizes the local symmetry of the system. Its behaviour as a function of temperature is presented in the right panel of figure 12: $\langle Q_3 \rangle$ is constant at low temperatures and show a steady decline above $T \approx 900$ for instantaneous configurations. Another set of orientational quantities, the Rey parameters, quantify the relative orientation between neighbouring tetrahedra. We found that one of the most frequent relative positions between tetrahedra was the 1–1 configuration. As shown in the left panel of figure 12, the corresponding parameter tends to the value of randomly oriented tetrahedra at high temperatures, increases upon lowering the temperature and finally stabilizes around $T \approx 1500$.

The fact that $\langle Q_3 \rangle$ is constant below T_g is not very surprising, it lies in the very definition of the glass transition temperature. However, the marked change in the Rey parameters observed at T_c is more interesting. The extraction of T_c requires an extrapolation from high temperature data; D only behaves as a power law as predicted by MCT down to some $T > T_c$. Our results in figure 6 clearly show this behaviour, where the measured value of D is actually different from zero at T_c. Moreover, around T_c the system was at equilibrium, e.g. no ageing effects were observed. This implies that the freezing in the Rey parameters at T_c is not a consequence of lack of thermalization at the time scales reached by the simulations. Then, we were able to observe a mode-coupling-like scenario and also to give an interpretation on the origin of the slowing down of relaxation at T_c for the metasilicate, namely, the freezing of orientational degrees of freedom.

The limitation of MCT in describing the glass transition is frequently attributed to the lack of 'hopping processes' in its

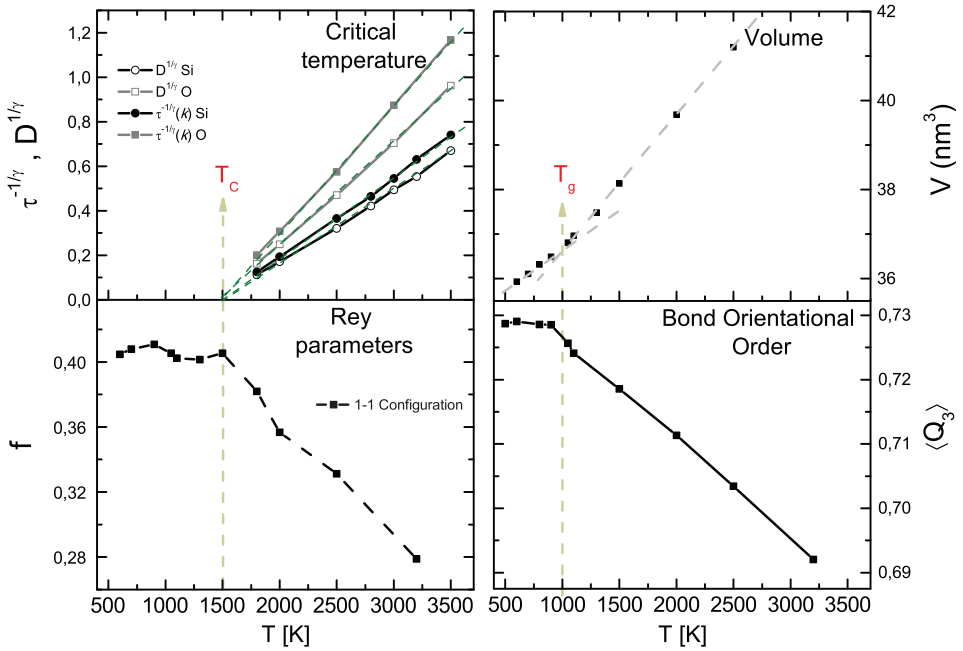

Figure 12. The four plots illustrate the presence of the two characteristic temperatures T_c and T_g at which dynamical and thermodynamical quantities show some sort of singularity, as explained in the text.

formulation, which are activated events that presumably grow in frequency around T_c and dominate the low T dynamics which preempts the glass transition [24]. Our work sheds light on this issue for more complex systems such as metasilicates: at T_g the degrees of freedom associated with the rotation of tetrahedra freeze, and the only source of relaxation remaining may come from O atoms jumping between different corners of tetrahedra. We have observed some support for this interpretation in our simulations. This could be further supported by the fact that $\langle Q_3 \rangle$ for inherent structures is constant for $T < T_c$. This could be a good starting point for future investigation of the presence of hopping processes in tetrahedron-forming systems.

To finish, we note that the existence of two separate temperatures, T_c and T_g, is certainly not exclusive to this system. It would be interesting to check if the present description in terms of orientational order parameters at local and medium distance scales may apply in different models of glasses. For systems that form tetrahedra the application of this idea would be straightforward. However, for simpler models such as the popular Lennard-Jones binary mixture, the identification of the relevant orientational degrees of freedom, if they exist at all, is more of a challenge.

Acknowledgments

We thank A C Angell for comments in the early stages of this work and T Grigera for discussions about the interpretation of the results. The Brazilian agency *Conselho Nacional de Desenvolvimento Científico e Tecnológico* (CNPq) is acknowledged for partial financial support.

References

[1] Greaves G N and Sen S 2007 *Adv. Phys.* **56** 1
[2] Dyre J C, Maass P, Roling B and Sidebottom D L 2009 *Rep. Prog. Phys.* **72** 046501
[3] Lammert H and Heuer A 2010 *Phys. Rev. Lett.* **104** 125901
[4] Horbach J, Kob W and Binder K 2002 *Phys. Rev. Lett.* **88** 125502
[5] Berthier L and Biroli G 2011 *Rev. Mod. Phys.* **83** 587
[6] Sastry S and Angell C A 2003 *Nature Mater.* **2** 739
[7] Tanaka H 2012 *Eur. Phys. J.* E **35** 113
[8] Götze W 1999 *J. Phys.: Condens. Matter* **11** A1
[9] Biroli G and Bouchaud J-P 2012 *Structural Glasses and Supercooled Liquids: Theory, Experiment, and Applications* (New York: Wiley)
[10] Berthier L and Tarjus G 2010 *Phys. Rev.* E **82** 031502
[11] Steinhardt P J, Nelson D R and Ronchetti M 1983 *Phys. Rev.* B **28** 784
[12] Rey R 2007 *J. Chem. Phys.* **126** 164506
[13] Ida Y 1976 *Phys. Earth Planet. Inter.* **13** 87
[14] Allen M P and Tildesley D 1987 *Computer Simulation of Liquids* (Oxford, UK: Oxford University Press)
[15] Frenkel D and Smit B 1986 *Understanding Molecular Simulation: from Algorithms to Applications* 2nd edn (San Diego, CA: Academic Press)
[16] Habasaki J and Okada I 1992 *Mol. Simul.* **9** 319
[17] Heuer A, Kunow M, Vogel M and Banhatti R D 2002 *Phys. Chem. Chem. Phys.* **4** 3185
[18] Banhatti R D and Heuer A 2001 *Phys. Chem. Chem. Phys.* **3** 5104
[19] Ispas S, Charpentier T, Mauri F and Neuville D R 2010 *Solid State Sci.* **12** 183192
[20] Plimpton S J 1995 *J. Comput. Phys.* **1** 117
[21] Balbuena C, Frechero M A and Montani R A 2013 *J. Non-Cryst. Solids* **369** 17
[22] Habasaki J and Hiwatari Y 2004 *Phys. Rev.* B **69** 144207
[23] Horbach J and Kob W 2002 *J. Phys.: Condens. Matter* **14** 9237
[24] Flenner E and Szamel G 2013 *J. Chem. Phys.* **138** 12A523
[25] Cates M E and Ramaswamy S 2006 *Phys. Rev. Lett.* **96** 135701
[26] Tang T and Luo D-L 2010 *J. At. Mol. Sci.* **1** 185
[27] Wang Z Q and Stroud D 1991 *J. Chem. Phys.* **94** 3896